New NMR Methods for the Characterization of Bound Waters in Macromolecules

Richard W. Kriwacki,† R. Blake Hill,† John M. Flanagan,‡,§ John P. Caradonna,† and James H. Prestegard*,†

Contribution from the Department of Chemistry and Department of Molecular Biophysics and Biochemistry, Yale University, New Haven, Connecticut 06511

Received April 1, 1993®

Abstract: The study of water molecules which are associated with macromolecules, either at the surface or buried within the interior, is important because these waters play significant structural, catalytic, and/or recognition roles. We demonstrate new NMR techniques that will allow the determination of the lifetimes of certain bound water molecules. These techniques employ (i) pulsed field gradients (PFG) for diffusion editing, (ii) isotope editing for selective detection and solvent suppression, and (iii) selective excitation for efficiency of acquisition. Using a uniformly ^{15}N-labeled fragment of the *Escherichia coli* chaperone protein, DnaJ, we show that a range of exchange lifetimes is observed for protons that physically exchange between water and amide sites. These methods will similarly allow the differentiation of bound water molecules on the basis of their lifetimes in the bound state and will be of general utility in the future for detailed studies of the dynamics of bound waters that have lifetimes in the 100 μs to 10 ms range.

The study of water molecules associated with the surface, or buried within the interior, of biological macromolecules is important for a number of reasons. Interactions at the macromolecular surface clearly play a role in defining the thermodynamically most stable structure;[1,2] waters in the interior of catalytically active proteins are known to participate directly in enzyme mechanisms;[3,4] and bound waters in the grooves of nucleic acid helices may well contribute to the topology recognized by proteins.[3-8] Much effort has therefore been directed at the kinetic and structural characterization of these water molecules. High-resolution X-ray structures of protein and nucleic acid crystals[8-12] have identified large numbers of tightly bound water molecules, and multidimensional NMR[13] methods have contributed to dynamic information on water molecules and have extended solid-state structural information to the solution phase.[14-20]

The investigation of bound water molecules by NMR techniques has, until recently, been impeded by technical problems associated with distinguishing small numbers of discrete, bound water protons from the enormous number of protons in bulk solvent. Advances in water suppression techniques allowed some very important studies of non-isotopically labeled proteins[15,18] and nucleic acids.[20] However, recent studies have increasingly employed selective detection of protons bound to heteronuclei (^{13}C or ^{15}N) to improve suppression of bulk water signals.[14,19]

Experiments with uniformly ^{15}N-labeled proteins focus on amide protons which are both spin coupled to ^{15}N nuclei and free to interact with water protons. Cross peaks in 2D or 3D maps originating from physical exchange or spin–spin cross relaxation between protons of water and specific amide protons can be interpreted as evidence of water accessibility to ordered regions within a protein structure. While such studies are valuable in locating amide protons associated with water, they are only a coarse probe of the dynamic properties of these bound or surface-associated waters. For example, rapid amide proton exchange with protons represented by the bulk water resonance requires proximity of a water molecule to the amide site and exchange of that water with bulk at a rate sufficient to show an averaged chemical shift (>100 s^{-1}), but it says little about whether the involved water molecule is exchanging with bulk solvent at a rate of 100, 1000, or 10 000 s^{-1}.

With these issues in mind, we propose a series of experiments which (i) take advantage of existing isotope filtering methods, (ii) are optimized with regard to minimizing acquisition time, and (iii) extend existing methods by encoding bound water lifetime, or exchange rate, information in water resonance–amide resonance correlation signals. We first present experiments (Figure 1) which are designed to efficiently detect correlations with the water proton resonance (or other degenerate resonances) and enable us to classify the origin of the interactions as chemical exchange, cross relaxation, and/or scalar coupling. These experiments are based

† Department of Chemistry.
‡ Department of Molecular Biophysics and Biochemistry.
§ Current address: Biology Department, Brookhaven National Laboratory, Upton, NY 11973.
® Abstract published in *Advance ACS Abstracts,* August 15, 1993.

(1) Saenger, W. *Annu. Rev. Biophys. Biophys. Chem.* **1987**, *16*, 93–114.
(2) Teeter, M. M. *Annu. Rev. Biophys. Biophys. Chem.* **1991**, *20*, 577–600.
(3) Westhof, E. *Int. J. Biol. Macromol.* **1987**, *9*, 186–192.
(4) Westhof, E. *Annu. Rev. Biophys. Biophys. Chem.* **1988**, *17*, 125–144.
(5) Otwinowski, Z.; Schevitz, R. W.; Zhang, R. G.; Lawson, C. L.; Joachimiak, A.; Marmostein, R. Q.; Luisi, B. F.; Sigler, P. B. *Nature* **1988**, *335*, 321–329.
(6) Aggarwal, A. K.; Rodgers, D. W.; Drottar, M.; Ptashne, M.; Harrison, S. C. *Science* **1988**, *242*, 99–107.
(7) Rould, M. A.; Perona, J. J.; Soll, D.; Steitz, T. A. *Science* **1989**, *246*, 1135–1142.
(8) Steitz, T. A. *Q. Rev. Biophys.* **1990**, *23*, 205–279.
(9) Bernstein, F. C.; Koetzle, T. F.; Williams, G. J. B.; Meyer, J. E. F.; Brice, M. D.; Rodgers, J. R.; Kennard, O.; Shimanouchi, T.; Tasumi, M. *J. Mol. Biol.* **1977**, *112*, 535–542.
(10) Finney, J. L. In *Water, A Comprehensive Treatise*; Franks, F., Ed.; Plenum: New York, 1979; Vol. 6, pp 47–122.
(11) Edsall, J. T.; McKenzie, H. A. *Adv. Biophys.* **1983**, *16*, 53–183.
(12) Baker, E. N.; Huddard, R. E. *Prog. Biophys. Mol. Biol.* **1984**, *44*, 97–179.
(13) Abbreviations used: NMR, nuclear magnetic resonance; 2D, two-dimensional; 3D, three-dimensional; NOESY, nuclear Overhauser effect correlation spectroscopy; ROESY, rotating frame Overhauser effect correlation spectroscopy; HMQC, heteronuclear multiple quantum coherence correlation spectroscopy; PFG, pulsed field gradient; TOCSY, total correlation spectroscopy; ppm, parts per million; TSP, 3-(trimethylsilyl)propionic-2,2,3,3-d_4 acid, sodium salt.
(14) Clore, G. M.; Bax, A.; Wingfield, P. T.; Gronenborn, A. M. *Biochemistry* **1990**, *29*, 5671–5676.
(15) Otting, G.; Wüthrich, K. *J. Am. Chem. Soc.* **1989**, *111*, 1871–1875.
(16) Otting, G.; Liepinsh, E.; Wüthrich, K. *J. Am. Chem. Soc.* **1991**, *113*, 4363–4364.
(17) Otting, G.; Liepinsh, E.; Wüthrich, K. *Science* **1991**, *254*, 974–980.
(18) Otting, G.; Liepinsh, E.; Farmer, B. T., II; Wüthrich, K. *J. Biomol. NMR* **1991**, *1*, 209–215.
(19) Qian, Y. Q.; Otting, G.; Wüthrich, K. *J. Am. Chem. Soc.* **1993**, *115*, 1189–1190.
(20) Kubinec, M. G.; Wemmer, D. E. *J. Am. Chem. Soc.* **1992**, *114*, 8739–8740.

0002-7863/93/1515-8907$04.00/0

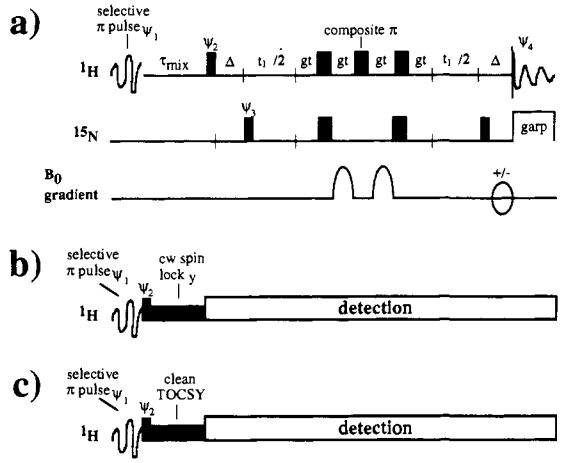

Figure 1. Pulse sequences used for selective PFG 2D (a) NOESY-HMQC, (b) ROESY-HMQC, and (c) TOCSY-HMQC experiments. The thin bold bars represent $\pi/2$ pulses; the thick bold bars represent π pulses. All pulse phases were along x unless otherwise shown. The composite sequence consists of $(\pi/2)_x$–π_y–$(\pi/2)_x$ pulses.

on previous 3D NOESY-HMQC,[21-23] 3D ROESY-HMQC,[14] and 3D TOCSY-HMQC[22-24] experiments but have been simplified through the use of (i) selective excitation of the water resonance[25-27] and (ii) pulsed field gradients (PFG) to select for amide protons coupled to ^{15}N nuclei.[28]

The introduction of selective water excitation acts to reduce the three-dimensional experiments to two-dimensional analogs that contain primarily information about water molecules. More precisely, the initial proton evolution period of a 3D NOESY-HMQC, 3D ROESY-HMQC, or 3D TOCSY-HMQC experiment is replaced with a frequency-selective 180° pulse centered on the H_2O resonance. The selective inversion pulse is followed by a mixing period, during which protons at the position of the water resonance interact with the protons of the protein through cross relaxation and/or chemical exchange (NOESY[29] and ROESY[30] mixing schemes) or through scalar coupling (TOCSY[22,31,32] mixing schemes). Magnetization that is transferred from water to protein amide sites is then detected using a PFG-enhanced version of the HMQC pulse sequence.[28] The PFG enhancement offers virtual elimination of the H_2O resonance during the detection period without the need for presaturation or spin-locking procedures. Amide resonances that are correlated with the H_2O resonance are selectively detected by coadding free induction decays corresponding to one complete cycle of the pulse sequence (16 scans with cycled pulse phases) with the H_2O resonance inverted, followed by subtraction of an equal number of scans with the H_2O resonance unperturbed.[33] The resonances

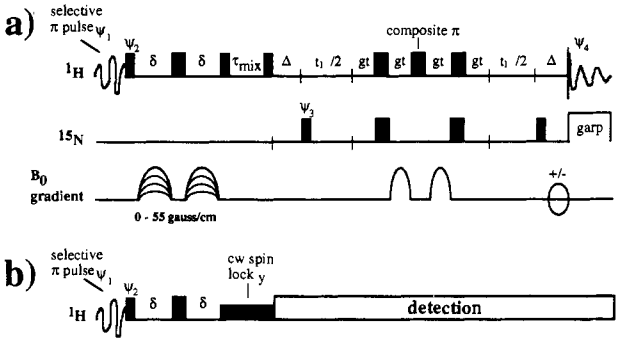

Figure 2. The pulse sequence used for the diffusion-filtered, selective PFG 2D NOESY-HMQC experiment. The thin bold bars represent $\pi/2$ pulses; the thick bold bars represent π pulses. All pulse phases were along x unless otherwise shown. The composite sequence consists of $(\pi/2)_x$–π_y–$(\pi/2)_x$ pulses. The corresponding PFG 2D ROESY-HMQC sequence involves replacement of the mixing period, τ_{mix}, and the two flanking $\pi/2$ pulses by a continuous wave spin-lock along the y-axis (B_1 = 5 kHz).

observed in these selective difference spectra must arise from magnetization originating on H_2O (or a degenerate resonance) that is transferred to amide protons through cross relaxation, scalar coupling, and/or physical exchange. This selective approach allows efficient acquisition of the several types of spectra (NOESY, ROESY, TOCSY) required for detailed interpretation of correlations between H_2O and amide resonances in a time comparable to that needed for a single plane of a 3D experiment.

Next we present a modification of the sequence for the NOESY and ROESY experiments, which includes PFG spin-echo techniques first used by Torrey[34] and Stejskal and Tanner.[35] These techniques are implemented in the form of a "diffusion-rate filter", similar to that utilized in the DRYCLEAN experiment developed by Van Zijl and Moonen,[36] which allows the H_2O magnetization, after selective inversion, to be filtered on the basis of diffusion rate and for this diffusion-rate information to be transferred to the detected amide resonances (see Figure 2). These new techniques are designed to differentiate among water molecules showing correlations with amide protons (through cross relaxation and/or chemical exchange) on the basis of their rate of exchange with bulk H_2O.

The PFG diffusion filter consists of B_0 field gradients applied during two periods (δ) separated by a single refocusing 180° pulse (Figure 2). After the application of this echo sequence, the protons of slowly diffusing molecules (i.e. macromolecules) will be refocused, while rapidly diffusing molecules (i.e. bulk water) will not. In this way, spectra can be edited to select peaks arising from slowly diffusing species. The filter can be adjusted to select signals originating from groups of waters displaying progressively smaller effective diffusion coefficients by increasing either the gradient strength or the time interval (2δ). As the result of this association with (or chemical exchange with) proteins, effective diffusion constants for water can vary over a range of 1 or 2 orders of magnitude. In the limit where exchange between bound and bulk waters is very fast compared to the time interval of the diffusion filter, the observed diffusion constant is essentially a weighted average of the diffusion constants of the bound and bulk states. Due to the preponderance of bulk water, the effective diffusion constant will be that of bulk water. In the limit where exchange is very slow compared to the filter duration, the effective diffusion constant will approach a value equal to that of the protein.

We have performed initial tests of this new methodology using an ^{15}N-labeled protein fragment (amino acids 1–78) derived from

(21) Fesik, S. W.; Zuiderweg, E. R. P. *J. Magn. Reson.* **1988**, *78*, 588–593.
(22) Marion, D.; Kay, L. E.; Sparks, S. W.; Torchia, D. A.; Bax, A. *J. Am. Chem. Soc.* **1989**, *111*, 1515–1517.
(23) Kay, L. E.; Marion, D.; Bax, A. *J. Magn. Reson.* **1989**, *84*, 72–84.
(24) Marion, D.; Driscoll, P. C.; Kay, L. E.; Wingfield, P. T.; Bax, A.; Gronenborn, A. M.; Clore, G. M. *Biochemistry* **1989**, *28*, 6150–6156.
(25) Shinnar, M.; Elff, S.; Subramanian, H.; Leigh, J. S. *Magn. Reson. Med.* **1989**, *12*, 75–80.
(26) LeRoux, P. In *Proc. Magn. Reson. Med., 7th Annu. Meeting*; Raymond, A. E., Ed.; Academic Press: San Diego, 1988; p 1049.
(27) John, B. K.; Plant, D.; Webb, P.; Hurd, R. E. *J. Magn. Reson.* **1992**, *98*, 200–206.
(28) Tolman, J. R.; Chung, J.; Prestegard, J. H. *J. Magn. Reson.* **1992**, *98*, 462–467.
(29) Ernst, R. R.; Bodenhausen, G.; Wokaun, A. *Principles of Nuclear Magnetic Resonance in One and Two Dimensions*; Clarendon/Oxford: New York, 1987.
(30) Bothner-By, A. A.; Stephens, R. L.; Lee, J.; C. Waren, D.; Jeanloz, R. W. *J. Am. Chem. Soc.* **1984**, *106*, 811–813.
(31) Braunschweiler, L.; Ernst, R. R. *J. Magn. Reson.* **1983**, *53*, 521–528.
(32) Griesinger, C.; Otting, G.; Wüthrich, K.; Ernst, R. R. *J. Am. Chem. Soc.* **1988**, *110*, 7870–7872.
(33) Hall, L. D.; Sanders, J. K. M. *J. Am. Chem. Soc.* **1980**, *102*, 5703–5711.
(34) Torrey, H. C. *Phys. Rev.* **1956**, *104*, 563–566.
(35) Stejskal, E. O.; Tanner, J. E. *J. Chem. Phys.* **1965**, *42*, 288–292.
(36) Van Zijl, P. C. M.; Moonen, C. T. W. *J. Magn. Reson.* **1990**, *87*, 18–25.

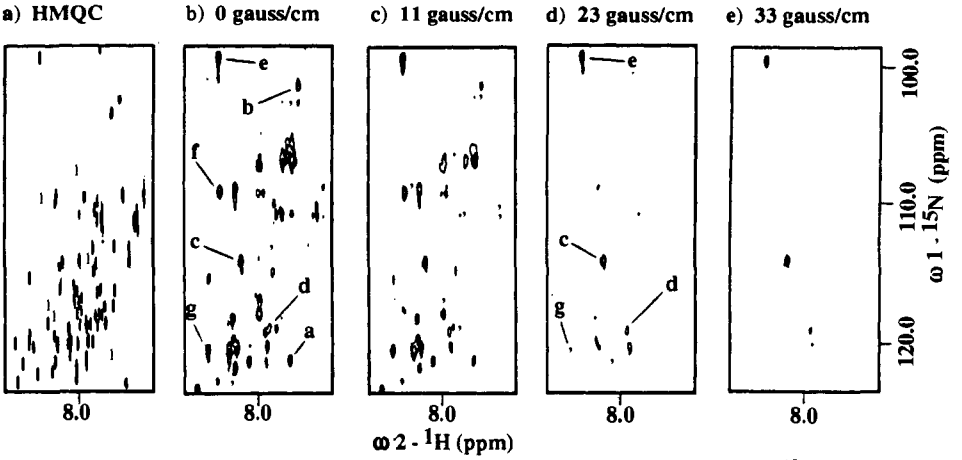

Figure 3. Results of the diffusion-filtered, selective PFG 2D NOESY-HMQC experiment for the uniformly ^{15}N-labeled DnaJ fragment: (a) 2D PFG HMQC spectrum for reference; (b) diffusion-filtered spectrum with gradient strength 0 G/cm; (c) 11 G/cm; (d) 23 G/cm; and (e) 33 G/cm. Peaks labeled a–g in panel b are discussed in detail in the text.

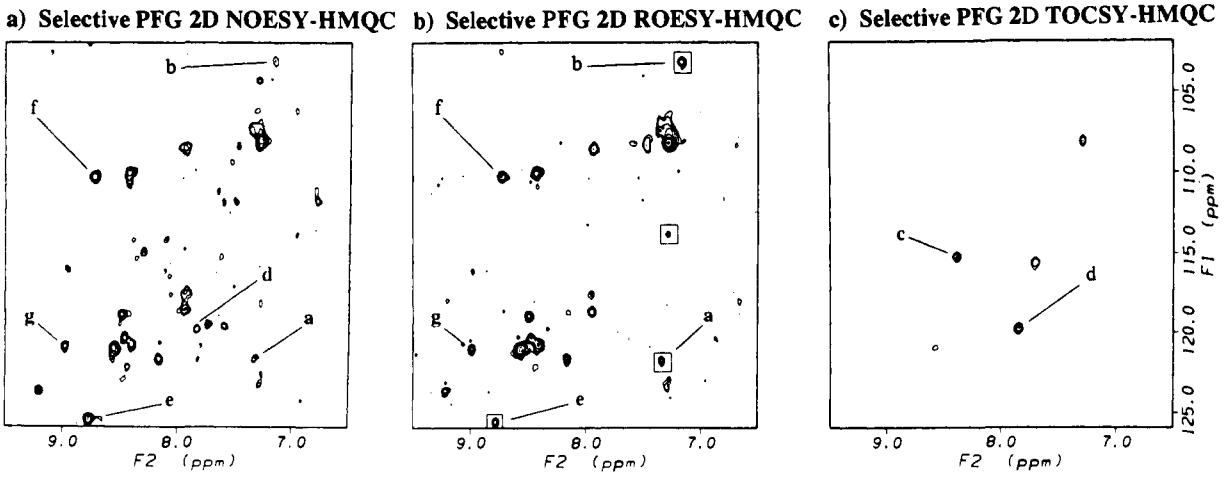

Figure 4. Results for selective PFG 2D (a) NOESY-HMQC, (b) ROESY-HMQC, and (c) TOCSY-HMQC experiments for the DnaJ fragment. These data were used to establish the categorization of peaks labeled a–g in Figure 3b and are discussed in detail in the text.

the *Escherichia coli* heat shock protein, DnaJ (376 amino acids).[37] DnaJ, in concert with DnaK (*E. coli* Hsp70), is known to be involved in a wide variety of cellular processes, ranging from phage replication and cell division to protein processing and translocation.[38,39] Additionally, the DnaJ/DnaK pair have been shown in vitro to be involved in chaperone-mediated protein folding.[40] The DnaJ/DnaK pair are thought to bind to nascent polypeptide chains and maintain them in a folding competent state prior to their GrpE dependent transfer to GroEL/GroES, where the final steps in chaperone-mediated folding occur.

The 78-residue DnaJ polypeptide examined in this study contains the "DnaJ homology domain" corresponding to the most highly homologous portion of the amino acid sequence.[39] In fact, this is the single domain that is common to both DnaJ and SEC63, an integral membrane protein involved in transit of nascent secretory proteins across the endoplasmic reticulum.[40] The highly conserved nature of this region of DnaJ suggests that it may play an important role in its function.

Results

Figure 3b–e shows the results for a series of experiments acquired using the diffusion-filtered, selective NOESY-HMQC sequence (Figure 2a) at increasing gradient strengths using the ^{15}N-labeled DnaJ fragment. For comparison, a normal 2D HMQC[41] spectrum is shown in Figure 3a, which contains one peak for each amide in the protein. Clearly, only a subset of the amides exhibit correlations with water (or some other proton at the water frequency); moreover, these peaks display a wide variation in sensitivity to the gradient filter. Gradient strengths in Figure 3b–e were chosen to attenuate the water resonance by the factors 1.00, 0.67, 0.17, and 0.03 (corresponding to gradient amplitudes of 0, 11, 23, and 33 G/cm, respectively);[34,35] resonances from the slowly diffusing protein were only slightly affected over this range (data not shown). Most of the resonances appearing in Figure 3b–e can be grouped into one of three categories on the basis of results from selective NOESY-, ROESY-, and TOCSY-HMQC experiments (those sequences lacking the diffusion filter; pulse sequences given in Figure 1, 2D spectra shown in Figure 4). Peaks assigned to category I arise from bound water proton–amide proton spin–spin cross relaxation (positive NOESY peaks, negative ROESY peaks,[30] no TOCSY peaks). Peaks in category II arise from water proton–amide proton exchange (positive NOESY and ROESY peaks,[30] no TOCSY peaks). And finally, peaks in category III arise from α-proton–amide proton cross relaxation as the result of degeneracy of the α-proton resonance with that of water (positive NOESY and TOCSY peaks, weak positive ROESY peaks as the result of Hartmann–Hahn trans-

(37) Bardwell, J. C.; Till, A. K.; Craig, E.; King, J.; Zylicz, M.; Georgopoulos, C. *J. Biol. Chem.* **1986**, *261*, 1782–1785.
(38) Langer, T.; Lu, C.; Echols, H.; Flanagan, J.; Hayer, M. K.; Hartl, F. U. *Nature* **1992**, *356*, 683–689.
(39) Bork, P.; Sander, C.; Valencia, A.; Bukau, B. *Trends Biochem. Sci.* **1992**, *17*.
(40) Sadler, I.; Chiang, I.; Kurihara, T.; Rothblatt, J.; Way, J.; Silver *J. Cell Biol.* **1989**, *109*, 2665–2675.
(41) Bendall, M. R.; Pegg, D. T.; Doddrell, D. M. *J. Magn. Reson.* **1983**, *52*, 81–117.

fers). An additional category of peaks not observed with the DnaJ fragment studied here but observed in other studies[14,15,20] is characterized by negative NOESY peaks, negative ROESY peaks, and no TOCSY peaks. This category corresponds to cross relaxation between protons of water molecules with short correlation times (such that $\omega\tau_c < 1$) and amide protons.

Several examples of peaks within each of these categories are found in the series of spectra in Figure 3b–e. The peaks labeled a and b in Figure 3b belong to category I (bound water protons cross-relaxing with amide protons) and appear to decay rapidly as the gradient strength is increased. The bound water molecules responsible for these two peaks must (i) exchange between the bound and free states on a time scale that is short in comparison with the filter interval and (ii) exhibit the diffusion properties of bulk water. Peaks g and f belong to category II (water protons physically exchanging with amide protons) and display different exchange rates; peak g persists in the spectrum acquired with a gradient strength of 23 G/cm (Figure 3d), while peak f does not. Peaks c and d (category III) prove to arise from cross relaxation between DnaJ(1–78) α-protons degenerate with the water resonance and amide protons. TOCSY peaks corresponding to c and d are observed (Figure 4c). Both peaks are attenuated only slightly by the gradient filter, in agreement with these peaks arising from the slowly diffusion protein species. Peak e seems to belong to category III, since it exhibits the same dependence on gradient strength as peaks c and d and, therefore, must diffuse slowly. However, no TOCSY peak corresponding to an α-proton is observed, and therefore, the possibility that this peak is due to a long-lived bound water molecule cannot be excluded. We should also note that in Figure 3a–e peak e is aliased due to selection of a narrow spectral width; its true ^{15}N chemical shift, as seen in the spectra of Figure 4, is 126 ppm.

Discussion

We have, therefore, demonstrated efficient NMR techniques that allow the detection of H_2O–amide proton correlations. These techniques also allow the collection of information on the diffusional properties of water molecules giving rise to these correlations and in the future should allow detailed studies of water molecules that exchange slowly with, and/or are tightly associated with, protein amide protons. In order for the latter to be true, the exchange processes must occur on the time scale of the diffusion-filtered pulse sequence. Our results indicate a differential sensitivity to gradient amplitude even with the rather long diffusion filter period used here (14 ms). Most cross peaks in Figure 3b, corresponding to zero gradient strength, are significantly attenuated with the application of low-amplitude gradient pulses (Figure 3c). These attenuated peaks must correspond to amides that exchange with rapidly diffusing water molecules with an apparent diffusion constant near that of bulk water. However, a significant number of cross peaks persist at higher gradient strength (Figure 3d,e), with only a few of these clearly originating from nonexchangeable α-proton protein peaks. The prevailing picture of water near the surface of a protein is one in which movement (diffusion) is rapid.[17] Bulk water–bound water exchange times derived from spin relaxation[17] and exchange[16] studies are estimated to lie within the range 10^{-8}–10^{-2} s. We apparently observe water molecules with exchange times at the slow exchange extreme of this range.

While very tightly bound water molecules would seem the simplest explanation for such slow exchange, there are alternate explanations. Exchange of protons to other non-amide sites (i.e. hydroxyl sites) followed by cross relaxation with amide protons has been identified as an alternative mechanism, giving rise to H_2O–amide correlation peaks.[14,15] This process can significantly slow apparent bulk water–bound water exchange rates. However, it is also true that a diffusion filter probes translational mobility over a relatively long diffusional distance ($\sim 10^{-5}$ cm), while spin–spin relaxation, the dominant probe of mobility in previous studies, addresses translational or rotational mobility over very short distances ($\sim 10^{-7}$ cm). Water molecules that move, but do not easily escape from occluded regions in a protein, may also give apparently small diffusion constants. Thus, the difference in these two distance scales may lead to observed differences in the behavior of water molecules, as probed by the two different types of NMR phenomena.

The experiments presented are highly amenable to quantitation of both amide exchange rate and bulk water–bound water exchange rates and are limited only by the duration of the shortest possible effective gradient interval (currently $\sim$50–100 μs). Reduction of three-dimensional experiments to two dimensions saves considerable time and allows systematic incrementation of either exchange mixing times (τ_{mix}) or diffusion filter times (2δ), so that exchange rates can be quantitated. While applied in this report to an isotopically labeled protein sample, these techniques would be directly applicable to the study of waters associated with other classes of macromolecules that can be readily isotopically labeled. A quantitative analysis of proton exchange between H_2O and a small molecule using PFG exchange spectroscopy was recently reported by Moonen et al.,[42] and these methods, for exchange processes on the time scale of 10's to 100's of milliseconds, offer an alternative to those demonstrated in this report.

It is clear that a systematic investigation of water exchange times by the diffusion-filtered methods will be interesting and may lead to a better understanding of the functional/structural role of water at macromolecular surfaces and within their interiors. Because the three-dimensional structure of the 78 amino acid DnaJ fragment is not known, the information acquired here cannot be used immediately in structure-based interpretations, but it will likely be of use in defining the structure.

Experimental Section

^{15}N-Labeled DnaJ(1–78) was overexpressed in *E. coli* grown in MOPS minimal media containing $^{15}NH_4Cl$ as the sole nitrogen source.[43] DnaJ(1–78) was purified from *E. coli* extracts by a combination of ion exchange chromatography on an SP column followed by hydroxyapatite chromatography and size exclusion chromatography (further details of the overexpression and purification of DnaJ(1–78) will be presented elsewhere). The protein is homogeneous, as judged by SDS-PAGE (20% Phast Gels, Pharmacia) followed by silver staining. The NMR sample was 4 mM in DnaJ(1–78) and was dissolved in 50 mM sodium phosphate, pH 6.0, in 90% H_2O/10% D_2O.

The selective PFG 2D NOESY-HMQC, ROESY-HMQC, and TOCSY-HMQC experiments were performed using the pulse sequences given in Figure 1a–c (results shown in Figure 4a–c). Selective inversion of the H_2O resonance is achieved through the use of a low-power, amplitude-modulated pulse train initially developed by Shinar and LaRoux[25,26] and later implemented by John *et al.*[27] The experimental parameters used were selective Shinnar–LaRoux pulse width, 50 ms;[25–27] δ, 7.00 ms; τ_{mix}, 80 ms; Δ, 4.5 ms; gt, 2 ms at 55 G/cm; t_1 acquisition time, 26 ms; t_2 acquisition time, 160 ms; dwell time in t_1, 780 μs; dwell time in t_2, 294 μs; data size in t_1, 32 complex points, extended by linear prediction to 42 points, and zero-filled to 64; data size in t_2, 128 zero-filled to 512; ψ_1, $4x$, $4y$, $4-x$, $4-y$; ψ_2, $2x$, $2-x$; ψ_3, x, $-x$; and ψ_4, x, $2-x$, x. Quadrature detection in t_1 is achieved by alternating the sign of the last gradient pulse for pairs of t_1 points.[28] Alternate sets of 16 transients were collected with the power for the selective pulse either on or off, with the phase of the receiver inverted for the second set of scans. After each scan, 10-ms spin lock purge pulses were applied along the x- and y-axes to dephase persistent magnetization, followed by a 1-s recovery delay. The duration of the gradient pulses during the detection period (Figures 1 and 2) can be reduced by replacing the initial and final gt delays with gradient pulses of negative amplitude and doubling the amplitude of the final gradient pulse. This modification leads to a reduction of gt from 2 to 1.5 ms, with a comparable level of water

(42) Moonen, C. T. W.; Van Gelderen, P.; Vuister, G. W.; Van Zijl, P. C. M. *J. Magn. Reson.* **1992**, *97*, 419–425.
(43) Niedhardt, F. C.; Bloch, P. L.; Smith, D. F. *J. Bacteriol.* **1974**, *119*, 736–747.

supression, and leads to spectra equivalent to those shown here (data not shown). All spectra were acquired at 30 °C with the ^1H carrier positioned at 7.8 ppm relative to TSP at 0.0 ppm and the ^{15}N carrier positioned at 116 ppm relative to ammonia at 0.0 ppm. All data processing was performed using the program FELIX (2.0) (Hare Research, Inc.). In Figures 1b,c and 2b the period labeled "detection", including gradient, ^1H, and ^{15}N pulses, was identical to that for Figure 1a. In Figure 1b additional parameters were spin lock time, 40 ms and spin lock rf field strength, 5 kHz. In Figure 1c a clean TOCSY[32] mixing sequence based on MLEV-17[44] was used with spin lock time, 50 ms, and rf field strength, 12.5 kHz.

The series of spectra shown in Figure 3b–e were obtained using the diffusion-filtered, selective PFG 2D NOESY-HMQC pulse sequence shown in Figure 2a. The experimental parameters used for these experimenst were similar to those used for the selective experiments given above; additional parameters were as follows: ψ_1, $4x$, $4y$, $4-x$, $4-y$; ψ_2, $x, x, -x, -x$; ψ_3, $x, -x, x, -x$; ψ_4, $x, -x, -x, x$. The intensities of the pulsed B_0 gradients were 0, 11, 23, and 33 G/cm for panels b–e of Figure 3, respectively. The HMQC spectrum shown in Figure 3a was recorded using only the PFG HMQC portion of the pulse sequence given in Figure 1a, with parameters as given above. The corresponding PFG 2D ROESY-HMQC sequence (Figure 2b) involves replacement of the mixing period, τ_{mix}, and the two flanking $\pi/2$ pulses by a continuous wave spin-lock along the y-axis (B_1 = 5 kHz). All sequences were implemented on a GE Omega 500 spectrometer equipped with an S-17 gradient accessory.

(44) Bax, A.; Davis, D. G. *J. Magn. Reson.* **1985**, *65*, 355–360.

Acknowledgment. We thank Dr. J. Chung at Yale (currently at UC, Riverside) for helpful discussion regarding the diffusion work. J.M.F. was a member of Dr. Donald Engelman's laboratory, and we would like to gratefully acknowledge his contributions of laboratory space and encouragement. This work was supported by U.S. Public Health Service Grants GM48396 (to J.P.C.), GM32243 (to J.H.P.), and GM39546 (to J.M.F.), NSF Grant DMB-8805587 (to J.M.F.), NIH Predoctoral Biophysical Fellowship 5 T32 GM08293-04 (to R.W.K.), New Graduate Assistance Program in Chemistry P200A00228-91 (to R.W.K.), and a grant from the Heyl Foundation (to R.B.H.). This work also benefited from instrumentation provided by the National Science Foundation, DIR 9015967.